

Analysis of Light Propagation in Thin-Film Solar Cells by Dual-Probe Scanning Near-Field Optical Microscopy

Stephan Lehnen, Ulrich W. Paetzold, Markus Ermes, Karsten Bittkau, Reinhard Carius

IEK5 – Photovoltaics, Forschungszentrum Jülich GmbH, Jülich, 52425, Germany

Abstract - In this study, light propagation in textured hydrogenated microcrystalline silicon ($\mu\text{-Si:H}$) thin-film solar cells is investigated on a sub-micron-scale by means of dual-probe scanning near-field optical microscopy (SNOM). Applying advanced modes of operation - exclusively available at dual probe SNOMs - light propagation is analyzed with subwavelength resolution. Measurements at $\mu\text{-Si:H}$ thin-film solar cells layer are presented visualizing the influence of local surface features on light propagation. Furthermore, the intensity decay of light guided inside the solar cell is mapped. The observed intensity decay agrees well with theory, verifying the validity of the method.

Index Terms – characterization, light-trapping, near-field microscopy, thin-films

I. INTRODUCTION

Light-trapping is essential in thin-film photovoltaic devices. In the past, numerous light-trapping concepts have been developed which use various techniques, e.g. photonic crystals [1], dielectric gratings [2], plasmonic gratings [3, 4], or randomly textured interfaces [5], to enhance the path of light and thereby the absorption of incident light in optically thin absorber layers. Commonly, the investigation of the performance of different light-trapping concepts is restricted to indirect methods, like the determination of the external quantum efficiency or absorption measurements. These experimental methods are limited to macroscopic information about averaged properties of a large device area but the influence of single surface features remains unknown. Subwavelength sized surface features have a major impact on light-trapping efficiency since they distinctly modify the transmission of light through the front-interface from the ambient to the solar cell and vice versa [5]. Therefore, both incoupling and outcoupling of light from and to the solar cell are influenced by subwavelength sized features. Hence, an experimental method is required which provides high optical resolution to investigate light-trapping on a microscopic scale.

Scanning Near-field Optical Microscopy (SNOM) meets the demands. In order to advance the characterization methods to the analysis of light propagation, we extended the conventional microscope setup [6,7] to dual-probe operation. A dual-probe SNOM has been developed to gain direct insight into the propagation of light in thin-film solar cells. Most importantly, the method allows for visualizing light propagation with subwavelength resolution. In this work, we present measurements of light propagation within a microcrystalline silicon ($\mu\text{-Si:H}$) thin-film solar cell. The

measurements reveal the influenced of local surface features on the distribution of light. The observed intensity decay is explained by a combination of different mechanisms.

II. EXPERIMENTAL DETAILS

The applied SNOM uses two structurally identical independent probes designated to local illumination or detection, respectively. During a measurement, one or both probes scan above the sample surface at constant distance. This way, the three-dimensional surface topography is determined, similar to the analysis by atomic force microscopy (AFM). In contrast to AFM measurements, an aluminum coated tapered glass fiber is used as scanning probe which allows for measuring the local light intensity at each position of the measurement. Due to the small size of the

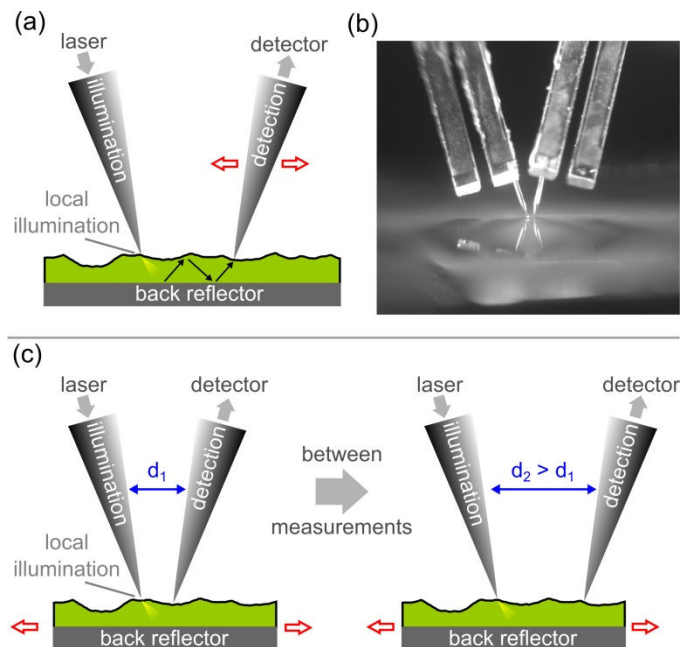


Fig. 1 (a) Illumination probe (left) and detection probe (right) in dual-probe configuration. The sample is locally illuminated by the illumination probe at a constant position while the detection probe scans the surrounding area. (b) Image of the probes attached to quartz tuning forks which are part of the shear-force distance control. (c) Extended dual-probe mode. During a measurement illumination and detection probe remain at constant distance while the sample is moved. The probe-to-probe distance is stepwise increased between the measurements. Two distance steps are displayed. In total, 25 steps covering the range from 3.5 μm to 16 μm are employed.

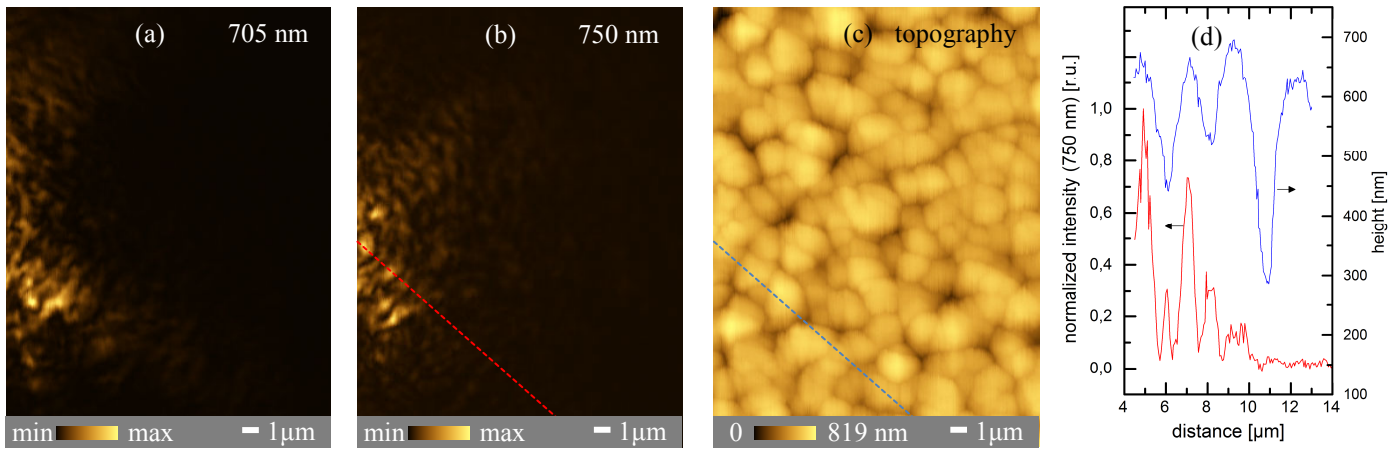


Fig. 2 Dual probe measurements at textured $\mu\text{c-Si:H}$ thin film solar cells measured at a wavelength of 705 nm (a) and 750 nm (b). The topography of the scan area is displayed in (c). A linescan of the measured intensity at 750 nm and the corresponding topography is shown in (d).

probe's aperture (~ 50 nm) and the short distance between probe and sample surface (~ 20 nm), subwavelength resolution (~ 80 nm) is achieved which outperforms by far the Abbe-limit of classical microscopy. The short probe-to-sample distance is realized by a shear-force mechanism [8] which provides the demanded accuracy and speed to avoid probe damage.

Although single-probe SNOMs are capable to determine local electromagnetic field intensities with high accuracy [9], the global illumination of a large sample area, which is applied at single probe SNOMs, results in a loss of information about the origin of the measured intensity at the detection probe. In order to investigate light propagation, the conventional setup of a single probe SNOM had to be extended by an additional probe. A dual-probe SNOM offers the unique feature to illuminate the sample locally with an illumination probe while an additional detection probe measures the light intensity at some distance to the illumination probe (Fig.1a,b). Both, illumination and detection take place on a subwavelength scale.

By using lock-in technique, the system is capable to operate with multiple wavelengths simultaneously. Up to six lasers with wavelengths ranging from 473 nm to 750 nm are aligned and coupled into the illumination probe. The measurements presented in this study are performed at wavelengths of 705 and 750 nm. Light at these wavelengths is only weakly absorbed in $\mu\text{c-Si:H}$ and light-trapping is particularly important.

Two modes of operation are employed. For the first and *conventional mode of operation*, the illumination probe is placed at a constant position on top of the investigated sample while the detection probe scans the surrounding area (Fig.1a,b). This mode of measurement is sensitive to local surface features. The so-called *extended mode of operation* uses a scan frame attached to the sample to move the sample underneath the probes which remain at constant distance to each other. Between multiple measurements the probe-to-probe distance is increased stepwise by 500 nm. In total, 25

successive measurements cover distances ranging from $3.5 \mu\text{m}$ to $16 \mu\text{m}$ (Fig.1c). A single measurement at a certain distance step displays the different coupling efficiencies between the probes. Although the probe-to-probe distance is kept constant within each single measurement, the probes are moved above a textured surface whereby the coupling efficiency depends on the local surface features underneath the probes. The measured light intensities at each distance step are averaged. This way, the averaged intensity decay of light propagating inside the $\mu\text{c-Si:H}$ solar cell is determined and characteristic features of this damping are analyzed.

Measurements were performed at a textured $\mu\text{c-Si:H}$ thin-film solar cell in substrate-configuration. The silicon absorber layer was deposited by PECVD and has a total thickness of about $1.1 \mu\text{m}$. The ZnO front interface has a thickness of 80 nm (Details are described in [2]).

III. EXPERIMENTAL RESULTS

The light propagation measured at a wavelength of 705 nm is shown in Fig. 2a. The sample was illuminated locally by the illumination probe placed at a constant position about $4.5 \mu\text{m}$ left of the displayed intensity map. The intensity was measured by the scanning detection probe. Fig. 2b displays the intensity distribution measured simultaneously at a wavelength of 750 nm. The measurements reveal that the light is not symmetrically distributed. Furthermore, the angular distribution as well as the occurrence of local bright spots with subwavelength diameter depends on the wavelength. Fig. 2d displays a Linescan which crosses the spots of the measurement at 750 nm. Additionally the corresponding height profile alongside the selected linescan is shown. The linescan exposes a continuous decay in intensity with a superimposing fine structure induced by the irregular crater like etched surface texture. A comparison of the intensity and the topography alongside the selected line reveals the known correlation of high light intensities at the edges of the topography [6].

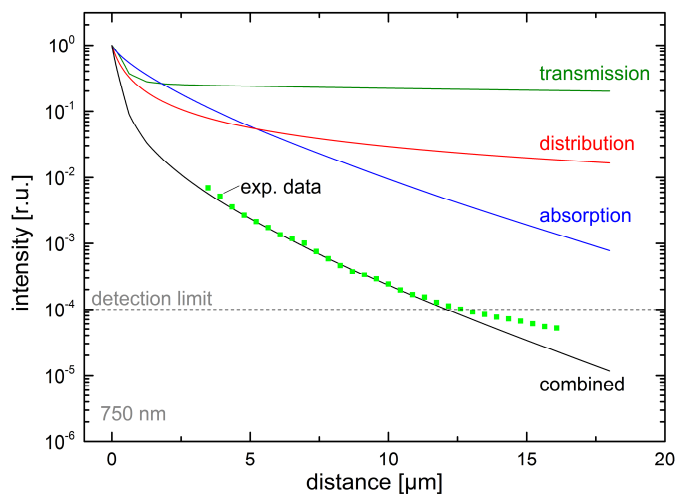


Fig. 3 Simulated intensity decay within a 1.1 μm thick layer of $\mu\text{c-Si:H}$ at a wavelength of 750 nm due to transmission at the front interface, distribution inside the layer and absorption besides experimental data determined by a dual-probe measurement.

The observed intensity decay of light with increasing distance to the origin of illumination is based on multiple mechanisms. Provided that the layer is thick compared to the wavelength of light inside the material, three aspects need to be considered to explain a decrease in intensity: (i) distribution, (ii) absorption and (iii) outcoupling of light at the front interface (transmission).

By means of a ray-tracing approach, the influence of the different loss-mechanisms¹ on the intensity decay inside the layer is investigated. Figure 3 displays the calculated relative strength of the intensity decay mechanisms besides experimental data.

The ray-tracing simulations show that at short distances, the distribution of light inside the layer is the main reason for the decrease in intensity. A major share of the light, emitted by the illumination probe, does not propagate in the direction towards the detection probe. Assuming that the illumination probe emits light radial symmetrically, the share in emitted light intensity, which is emitted in the direction towards the aperture of the detection probe, corresponds to a circle segment with the size of the probe's aperture. Hence, even if no other losses would exist at all, there is still a loss in the measured light intensity at the detection probe simply by a distribution of the light intensity inside the layer. If the light-guiding layer is thin in comparison to the minimal probe-to-

¹ Within the context of the investigation of light propagation inside a layer, all mechanisms which reduce the number of detected photons in a dual probe experiment are considered to be loss-mechanisms. However, this does not necessarily mean that they reduce solar cell performance. Indeed, absorption inside the absorber layer is a required process in solar cell operation. Likewise, the distribution of light inside the layer does in general not negatively affect the efficiency of a solar cell. In contrast outcoupling of light at the front interface actually reduces solar cell performance.

probe distance and has a high reflectivity at the front and back interfaces, the light can only propagate in two dimensions. It is confined to the xy-plane parallel to the sample surface. Hence, the intensity decreases reciprocally with the radius.

At long distances, the intensity is strongly decreased due to absorption. The intensity decay due to absorption displayed in Fig. 3 is based on the macroscopic value of the absorption coefficient of the applied $\mu\text{c-Si:H}$ layer (1387 cm^{-1} at 750 nm).

Furthermore, the intensity of light guided in the $\mu\text{c-Si:H}$ layer decreases by outcoupling through the front interface. In first approximation the reflection coefficient at the front interface is estimated by applying Fresnel equations. However, due to the rough interfaces, the transmission at the front interface likely differs. For example, light, incident at angles which exceed the angle of total reflection, can be scattered at a rough interface and thereby transmit through the front interface instead of being totally reflected.

The decrease in intensity and the relative strength between the loss-mechanisms depend on the angular distribution of light inside the layer. Implemented into solar cells, textured interfaces scatter the incident light into large angles [10, 11]. In a dual-probe experiment the angular distribution of light inside the sample layer is induced by the illumination probe. The angular emission characteristic of a SNOM probe is extracted from simulations (not shown) which allow access to the near-field behavior. Simulations reveal that the angular distribution of light emitted by a SNOM probe in near-field distance to the sample is comparable to the distribution induced by the commonly applied textured ZnO/ $\mu\text{c-Si}$ interfaces.

IV. FDTD SIMULATIONS

In order to confirm the experimental data and to gain insight into the electromagnetic field distribution inside the investigated layer, finite-difference time-domain (FDTD) simulations are performed. The simulated layer stack is equivalent to the measured samples. To realise open boundary conditions the stack is surrounded by a perfectly matched layer (PML) in all spatial directions. The illumination probe is modeled as a metalized glass cone with an opening angle of 15° , placed at a distance of about 50 nm above the ZnO layer. The aperture size is set to 160 nm. The light source is implemented as point source placed inside the probe. In correspondence to the experiment, the probe is tilted by 15° . In total, the simulation maps $10 \times 10\text{ }\mu\text{m}^2$ of the layer stack whereby the height is set to 8 μm .

A specific challenge is the large number of data points required to properly map the experimental system. On the one hand, a high resolution is necessary to take small features like the aperture into account. On the other hand, several micrometers of light propagation need to be simulated to allow for a comparison with the measurements.

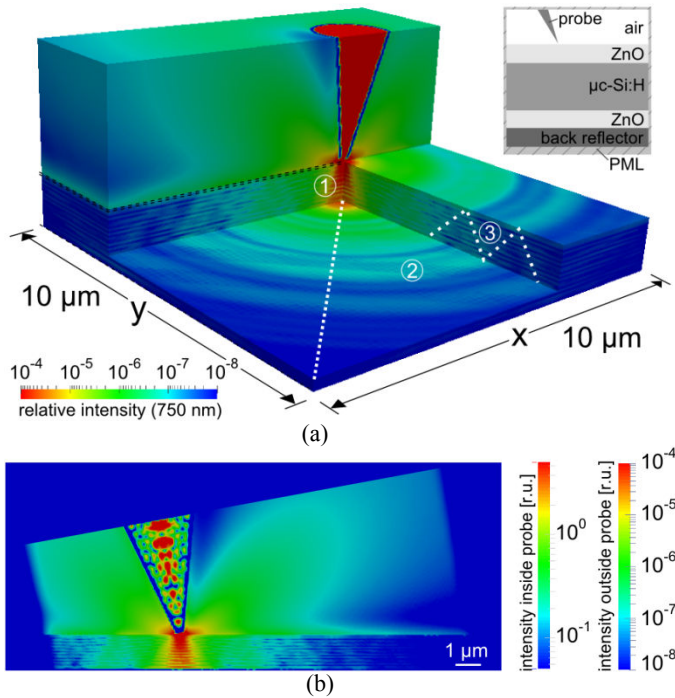


Fig. 4 (a) 3D visualization of the intensity distribution based on FDTD simulations. (b) Diagonal slice alongside the white dotted line in (a).

It is currently not feasible to include the detection probe in the simulation since a single simulation would be required for each distance step between illumination and detection probe. Instead, the intensity which corresponds to the experiment is extracted from the simulated intensity distribution at a height of 20 nm above the sample surface alongside the path the detection probes takes during an experiment.

Fig. 4(a) displays a 3D-visualization of the simulated intensity distributions for non-polarized light. The white dotted line corresponds to the direction the detection probe is moved during a dual-probe measurement. The intensity distribution at the diagonal plane crossing the white dotted line is displayed in Fig. 4(b).

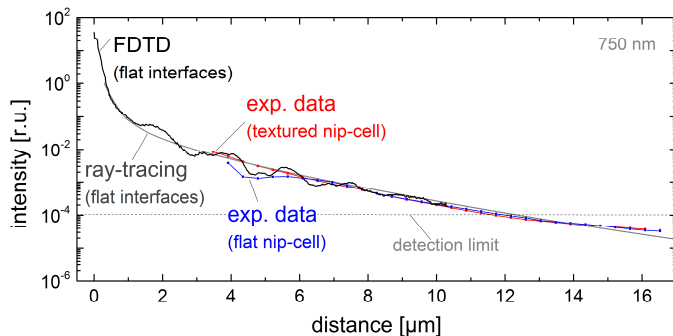


Fig. 5 Plot of the simulated intensity decay extracted 20nm above the surface alongside the white dotted line in Fig. 4a. For comparison, the intensity decay based on experimentally determined data is shown as well.

In Fig. 4(a), points of interest are marked with encircled numbers. The relative intensity directly underneath the aperture (1) is in the order of 10^{-4} . A loss of four orders of magnitude in intensity, depending on the aperture size, corresponds well to experiences from measurements. A distinct feature of the intensity distribution is a modulation of the intensity decay, visible as bright rings (2) at slices taken parallel to the sample surface. The modulations originate from interferences induced by multiple reflections of light inside the absorber layer (3). Whenever the light is reflected at the front interface, the local intensity is increased.

The modulation in intensity is also apparent in measurements of samples with flat surfaces, although scattering at small features of the nominally flat surface distort the modulation pattern at longer distances (Figure 5). Accordingly, measurements at samples with textured interfaces do not reveal any modulations of the intensity decay. The ray-tracing approach completely neglects the wave nature of light. Consequently, interferences do not occur in this model and a modulation of the intensity decay is not visible.

Despite of deviations between the simulated and the real probe structure, the ray-tracing as well as the FDTD simulations are in good agreement with the experimental results, demonstrating that the local light intensity distribution is successfully investigated by dual-probe SNOM, providing new insight into local influence of e.g. scattering and absorption.

IV. SUMMARY

We employ a newly developed dual-probe SNOM to determine successfully the light propagation in active solar cell layers. Dual-probe measurements performed at thin-film solar cells made of hydrogenated microcrystalline silicon reveal a continuous decay in intensity superimposed by subwavelength sized bright spots induced by the irregular surface texture.

Beyond this, we introduce an extended mode of operation for dual-probe measurement which compensates for the influence of surface features and reveals the characteristic intensity decay of light propagating inside the thin-film silicon solar cell.

The different mechanisms responsible for a decay in intensity of the propagating light are investigated by a ray-tracing approach which provides the relative strengths of the intensity decay induced by absorption, distribution inside the layer and transmission through the front interface.

Finally, the intensity decay of the propagating light, determined by FDTD simulations, revealed good accordance with the measured data. A modulation of the intensity decay, which originates from interference induced by multiple reflections, is observed in the measurement as well as in FDTD simulations.

REFERENCES

- [1] P. Bermel, C. Luo, L. Zeng, et al., "Improving thin-film crystalline silicon solar cell efficiencies with photonic crystals," *Optics Express*, 15(25):16986-17000, 2007.
- [2] C. Haase and H. Stiebig, "Optical properties of thin-film silicon solar cells with grating couplers," *Progress in Photovoltaics: Research and Applications*, 14(7): 629-641, 2006.
- [3] U. Paetzold, E. Moulin, D. Michaelis, et al., "Plasmonic reflection grating back contacts for microcrystalline silicon solar cells," *Applied Physics Letters*, 99(18), 2011.
- [4] P. Spinelli, V. E. Ferry, J. van de Groep, et al., "Plasmonic light trapping in thin-film Si solar cells," *Journal of Optics*, 14(2), 024002, 2012.
- [5] M. Berginski, J. Hüpkes, M. Schulte, et al., "The effect of front ZnO:Al surface texture and optical transparency on efficient light trapping in silicon thin-film solar cells," *J. Appl. Phys.*, vol. 101, 074903, 2007
- [6] K. Bittkau, R. Carius, C. Lienau, et al., "Guided optical modes in randomly textured ZnO thin films imaged by near-field scanning optical microscopy," *Phys. Rev. B*, 76: 035330, 2007.
- [7] G. Behme, A. Richter, M. Suptitz, et al., "Vacuum near-field scanning optical microscope for variable cryogenic temperatures," *Rev. Sci. Instrum.*, 68, 3458, 1997.
- [8] K. Karrai and R. Grober, "Piezoelectric Tip-sample Distance Control for Near-Field Optical Microscopes," *Applied Physics Letters*, 66(14):1842-1844, 1995.
- [9] K. Bittkau, T. Beckers, S. Fahr, et al., "Nanoscale investigation of light-trapping in a-Si:H solar cell structures with randomly textured interfaces," *Phys. Stat. Sol. A*, 205, 2766, 2008
- [10] M. Schulte, K. Bittkau, K. Jäger, et al., "Angular resolved scattering by a nano-textured ZnO/silicon interface," *Appl. Phys. Lett.*, 99, 111107, 2011
- [11] K. Bittkau, M. Schulte, M. Klein, et al., "Modeling of light scattering properties from surface profile in thin-film solar cells by Fourier transform techniques", *Thin Solid Film*, 519, 6538, 2011.